

Supplemental Material

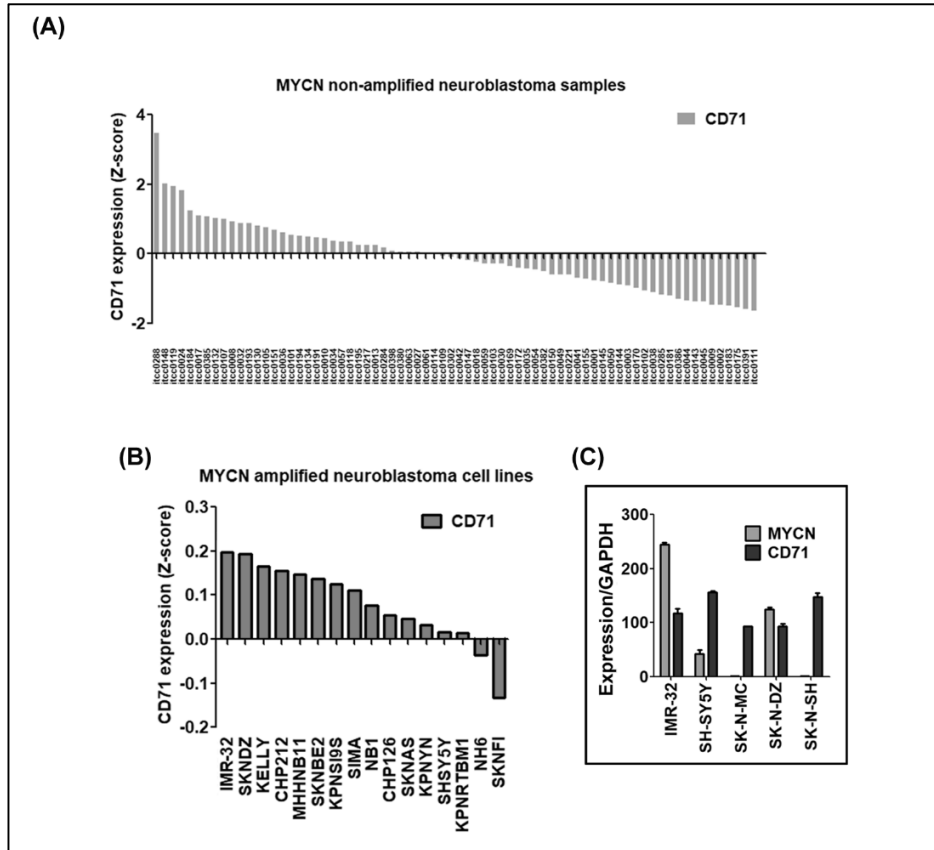
Targeting the Difficult-to-Drug CD71 and MYCN with Gambogic Acid and Vorinostat in a Class of Neuroblastomas

Kausik Bishayee Khadija Habib Ali Sadra Sung-Oh Huh

Department of Pharmacology, College of Medicine, Institute of Natural Medicine, Hallym University, Chuncheon, South
Korea

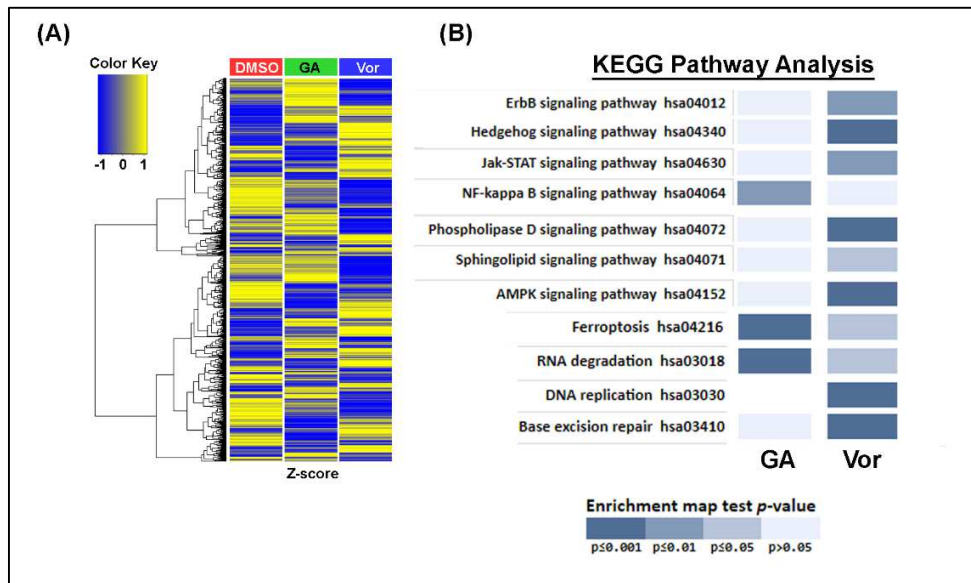
Supplementary figures

Suppl. Fig. 1



Suppl. Fig. 1. CD71 and MYCN expression in neuroblastoma patients and cell lines. (A) Expression of CD71 in MYCN non-amplified neuroblastoma patients were evaluated with the R2 platform and the AMC cohort “Neuroblastoma public-Versteeg-88” was used for this purpose. Expression levels of CD71 in MYCN non-amplified neuroblastoma patients were plotted in histogram form by using GraphPad Prism 5. (B) CD71 expression for the MYCN amplified neuroblastoma cells was plotted as a histogram by using GraphPad Prism 5. Expression data of neuroblastoma cell lines were obtained from CCLE dataset (The Cancer Cell Line Encyclopedia by Broad Institute, and the Novartis Institutes for Biomedical Research and its Genomics Institute of the Novartis Research Foundation, <http://www.broadinstitute.org>). (C) Expression of MYCN and CD71 was examined in IMR-32, SK-N-DZ, SH-SY5Y, SK-N-SH and SK-N-MC neuroblastoma cells by qPCR and plotted with GraphPad Prism 5. GAPDH was used to normalize the signals.

Suppl. Fig. 2 A-B



Suppl. Fig. 2. mRNA microarray analysis. (A) mRNA microarray analysis revealed differentially expressed mRNA in IMR-32 cells before and after GA and vorinostat treatment for 4 h. (B) Pathway enrichment was mapped after GA and vorinostat against DMSO control that indicated differential pathway activation via GA and vorinostat treatment.

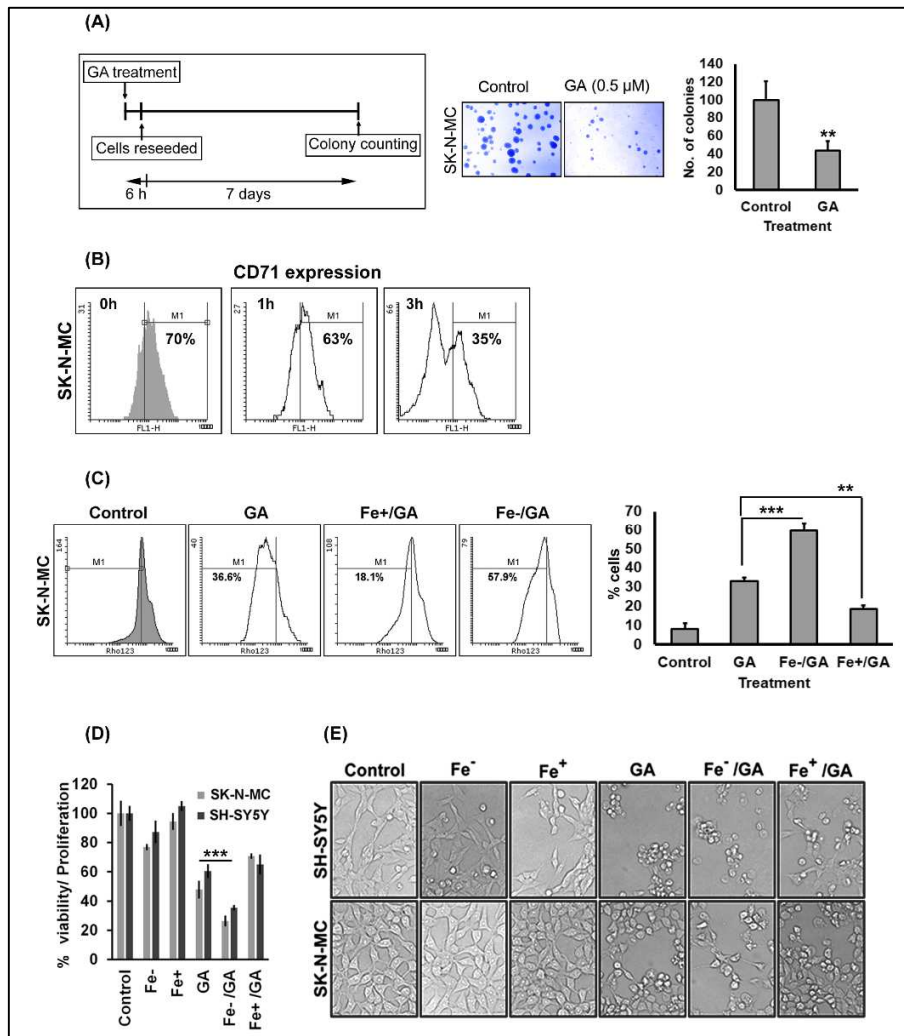
Suppl. Fig. 2 C

GA vs Control (KEGG pathway) p value<0.001			Vorinostat vs Control (KEGG pathway) p value<0.001		
Map ID	Map Name	Sig Genes	Map ID	Map Name	Sig Genes
04010	MAPK signaling pathway	40	01100	Metabolic pathways	147
05169	Epstein-Barr virus infection	33	04141	Protein processing in endoplasmic reticulum	47
05200	Pathways in cancer	45	05200	Pathways in cancer	71
04141	Protein processing in endoplasmic reticulum	29	04010	MAPK signaling pathway	55
05322	Systemic lupus erythematosus	26	04110	Cell cycle	39
05202	Transcriptional misregulation in cancer	29	04144	Endocytosis	44
05034	Alcoholism	28	05206	MicroRNAs in cancer	45
01100	Metabolic pathways	61	04218	Cellular senescence	34
03050	Proteasome	16	04024	cAMP signaling pathway	32
05206	MicroRNAs in cancer	29	05166	HTLV-I infection	35
04550	Signaling pathways regulating pluripotency of stem cells	21	05169	Epstein-Barr virus infection	31
05166	HTLV-I infection	24	04140	Autophagy - animal	25
05203	Viral carcinogenesis	20	05202	Transcriptional misregulation in cancer	29
04210	Apoptosis	17	04360	Axon guidance	28
04742	Taste transduction	14	04068	FoxO signaling pathway	25
04110	Cell cycle	16	05165	Human papillomavirus infection	36
05224	Breast cancer	17	04145	Phagosome	26
04218	Cellular senescence	16	05225	Hepatocellular carcinoma	27
04115	p53 signaling pathway	12	04115	p53 signaling pathway	19
04217	Necroptosis	15	04014	Ras signaling pathway	30

GA vs Control (GO function) p value<0.001			Vorinostat vs Control (GO function) p value<0.001		
GOID	Term	Count	GOID	Term	Count
GO:0005488	binding	967	GO:0005488	binding	1692
GO:0005515	protein binding	760	GO:0005515	protein binding	1354
GO:1901363	heterocyclic compound binding	499	GO:0097159	organic cyclic compound binding	827
GO:0097159	organic cyclic compound binding	503	GO:1901363	heterocyclic compound binding	818
GO:0003676	nucleic acid binding	376	GO:0043167	ion binding	778
GO:0043167	ion binding	446	GO:0003824	catalytic activity	709
GO:0003677	DNA binding	242	GO:0003676	nucleic acid binding	579
GO:0043169	cation binding	311	GO:0043169	cation binding	516
GO:0046872	metal ion binding	305	GO:0046872	metal ion binding	507
GO:0003824	catalytic activity	349	GO:0003677	DNA binding	358
GO:0001071	nucleic acid binding transcription factor activity	126	GO:0000166	nucleotide binding	341
GO:0003700	transcription factor activity, sequence-specific DNA binding	126	GO:1901265	nucleoside phosphate binding	341
GO:0003723	RNA binding	148	GO:0036094	small molecule binding	364
GO:0019899	enzyme binding	135	GO:0043168	anion binding	362
GO:0043168	anion binding	184	GO:0016740	transferase activity	323
GO:0043565	sequence-specific DNA binding	102	GO:0097367	carbohydrate derivative binding	317
GO:0044822	poly(A) RNA binding	109	GO:0035639	purine ribonucleoside triphosphate binding	281
GO:0097367	carbohydrate derivative binding	162	GO:0032550	purine ribonucleoside binding	281
GO:0030554	adenyl nucleotide binding	127	GO:0001883	purine nucleoside binding	281
GO:0032550	purine ribonucleoside binding	142	GO:0032549	ribonucleoside binding	281

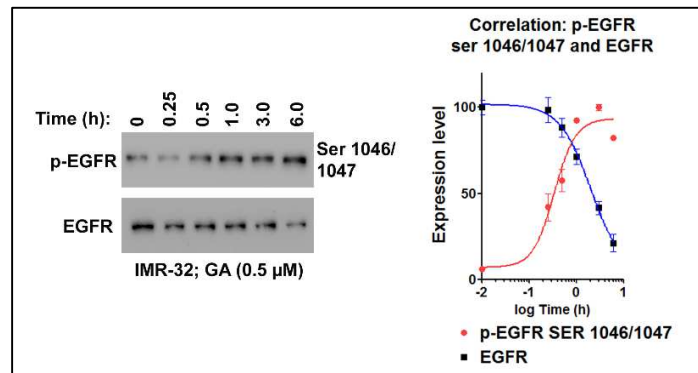
Suppl. Fig. 2. (C) Pathways from KEGG analysis that were uniquely altered by each treatment are shown along with their p-value of changes.

Suppl. Fig. 3



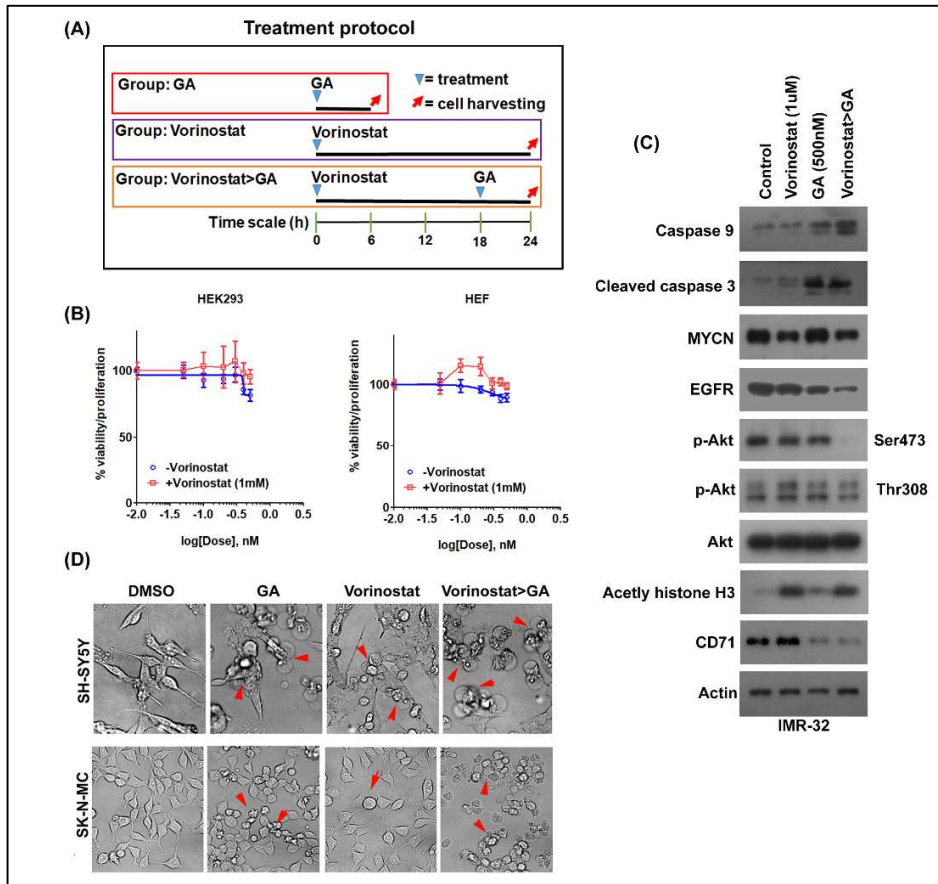
Suppl. Fig. 3. Gambogic acid treatment induces cell death. (A) SK-N-MC cells were treated with GA and incubated for 6 h and then washed and re-seeded in low attachment-6-well dishes at 100 cells per well and were monitored for 7 days to check for colony formation. The cell colonies were counted with crystal violet staining and plotted as histograms. (B) GA-treated SK-N-MC cells were stained with anti-CD71 antibody by indirect staining and analyzed in the FL-1H channel of the flow cytometer. The inserted histogram demonstrated a left shift of histogram peak after GA treatment after certain intervals with the percentage of cells (% cells) indicated. (C) GA-administrated SK-N-MC cells were harvested, fixed and stained with rhodamine 123. The inserted histogram demonstrated a left shift of histogram peak representing the decrease of rhodamine 123 fluorescence intensity due to the loss of MMP. Percentage of cells with reduced fluorescence intensity (M1) (% cells) was calculated. (D) Combined viability with proliferation read was via the MTT-assay and the relative percentage of viability with proliferation was calculated by the following formula: % viability, proliferation = (optical density (OD) of the drug-treated sample/OD of the control sample) × 100. The values were plotted as histograms. (E) Morphologies of SH-SY5Y and SK-N-MC cells were observed under an inverted light microscope at 20X magnification and digitally imaged.

Suppl. Fig. 4



Suppl. Fig. 4. Gambogic acid treatment induces EGF receptor phosphorylation at Ser1046/1047. IMR-32 cells were treated with 0.5 μ M of GA and incubated for the indicated time intervals. Expressions of p-EGFR Ser1046/1047 and EGFR were examined by Western blot. Expression densitometry was then plotted and curve fit was obtained using GraphPad Prism 5.

Suppl. Fig. 5



Suppl. Fig. 5. Vorinostat and gambogic acid modulate different growth and apoptotic signals. (A) Incubation time for vorinostat or panobinostat was 24 h and that for GA was 6 h. For combination treatment, cells were pretreated with vorinostat or panobinostat for 18 h before GA addition and were then incubated with GA for 6 h more. (B) The relative percentages of viability with proliferation were calculated by the following formula: % viability, proliferation = (optical density (OD) of the drug-treated sample/OD of the control sample) × 100. Values were plotted as a histogram by using GraphPad Prism 5. (C) Expression of different proteins were examined by Western blot after treatment. Actin was used as a loading control. (D) The morphology of neuroblastoma cells was examined after the treatments under an inverted microscope at 20X magnification. The red arrowheads are indicative of apoptotic cells.